

Electrokinetic Bioprocessor for Concentrating Cells and Molecules

Pak Kin Wong,[†] Che-Yang Chen,^{‡,§} Tza-Huei Wang,^{||} and Chih-Ming Ho^{*,†}

Institute for Cell Mimetic Space Exploration (CMISE) and Department of Mechanical & Aerospace Engineering, and Department of Biomedical Engineering, University of California, Los Angeles, Los Angeles, California 90095, and Department of Mechanical Engineering and Department of Biomedical Engineering, Johns Hopkins University, Baltimore, Maryland 21218

Bioprocessors for concentrating bioparticles, such as cells and molecules, are commonly needed in bioanalysis systems. In this microfluidic processor, a global flow field generated by ac electroosmosis transports the embedded particles to the regions near the electrode surface. The processor then utilizes electrophoretic and dielectrophoretic forces, which are effective in short range, to trap the target cells and molecules on the electrode surface. By optimizing the operating parameters, we have concentrated various biological objects in a large range of sizes, including *Escherichia coli* bacteria, λ phage DNA, and single-stranded DNA fragments as small as 20 bases that have a radius of gyration of only 3 nm.

Miniaturization of fluidic processes holds great potential for biochemical analysis systems. Automatic biomedical analysis with microfluidic systems eliminates labor-intensive benchtop processes and dramatically reduces the amount of sample and reagent required. This results in substantial reduction of both time and cost for the analysis. Fluid delivery, mixing with different reagents, and separation of different bioparticles are generic fluidic processes in biochemical analysis. For highly dilute samples, an effective collection procedure of targets such as bacteria or secreted molecules can significantly reduce the amount of fluid handling. In most cases, separation and concentration of targets from the sample can minimize noise and improve sensitivity. The efficiency of each fluidic operation in the sample preparation determines the overall performance of the biomedical analysis system.¹

Traditional methods of sample concentration include filtration, centrifugation, liquid–liquid extraction, and solid-phase adsorption.² Various techniques such as acoustic radiation pressure,³

microfabricated sieving filters,⁴ and evaporation-based concentration⁵ have been developed for concentrating target samples in microfluidic chips. These methods can be useful in some situations. However, they also have some drawbacks such as complex fabrication processes, long processing time, and integration difficulties with other fluidic components. Moreover, concentration of small biomolecules (in the order of nanometer) is especially challenging in a microfluidic system. On the other hand, electrokinetic manipulations of bioparticles are effective on the length scale of microfluidic systems^{6,7} and fabrication of microelectrodes is a relatively simple task. Electrokinetic forces have been demonstrated for enhancing mixing,⁸ performing sample separation,⁹ and improving detection efficiency¹⁰ in microfluidic systems. Therefore, it is advantageous to develop an electrokinetic processor that can be easily integrated with other electrokinetic components for collecting and concentrating a wide variety of targets.

Many different types of electrokinetic forces can be applied in microfluidic devices.⁷ Electrophoresis is the movement of charged particles in a liquid medium under an external electric field. Dielectrophoresis (DEP) describes the motion of polarizable particles under a nonuniform electric field. Ac electroosmosis generates bulk fluid motion on the electrode surface at frequency ranges below 1 MHz.¹¹ In this study, we exploit a combination of electrophoretic, dielectrophoretic, and ac electroosmotic forces for concentrating bioparticles. Ac electroosmotic force generates long-range fluid movement (Figure 1). The flow transports the embedded particles in the bulk fluid and pushes the particles to the electrode surface. The bulk fluid flow permits a large effective region for target concentration while other electrokinetic forces

* To whom correspondence should be addressed. Tel.: +1-310-825-9993. Fax: +1-310-206-2302. E-mail: chihming@ucla.edu.

[†] Institute for Cell Mimetic Space Exploration (CMISE) and Department of Mechanical & Aerospace Engineering, University of California.

[‡] Department of Biomedical Engineering, University of California, Los Angeles, Los Angeles, CA 90095.

[§] Current address: College of Law, University of Denver, Denver, CO 80208.

^{||} Department of Mechanical Engineering and Department of Biomedical Engineering, Johns Hopkins University, Baltimore, MD 21218.

(1) Ho, C.-M. In *Proc. IEEE MEMS '01*, Interlaken, Switzerland, 2001; pp 375–384.

(2) Belter, P. A.; Cussler, E. L.; Hu, W.-S. In *Bioseparations: Downstream Processing for Biotechnology*; Wiley: New York, 1988.

(3) Meng, A. H.; Wang, A. W.; White, R. M. In *Proc. Transducers '99*; Sendai, Japan, 1999; pp 876–879.

(4) van Rijn, C. J. M.; Nijdam, W.; Kuiper, S.; Veldhuis, G. J.; van Wolferen, H.; Elwenspoek, M. *J. Micromech. Microeng.* **1999**, *9*, 170–172.

(5) Walker, G. M.; Beebe, D. J. *Lab Chip* **2002**, *2*, 57–61.

(6) Pethig, R.; Markx, G. H. *Trends Biotechnol.* **1997**, *15*, 426–432.

(7) Wong, P. K.; Wang, T.-H.; Deval, J. H.; Ho, C.-M. *IEEE/ASME Trans. Mechatronics* **2004**, *9*, 366–376.

(8) Deval, J. H.; Tabeling, P.; Ho, C.-M. In *Proc. IEEE MEMS '02*, Las Vegas, NV, 2002; pp 36–39.

(9) Paegel, B. M.; Emrich, C. A.; Wedemayer, G. J.; Scherer, J. R.; Mathies, R. A. *Proc. Natl. Acad. Sci. U.S.A.* **2002**, *99*, 574–579.

(10) Wang, T.-H.; Wong, P. K.; Ho, C.-M. In *Proc. IEEE MEMS '02*, Las Vegas, NV, 2002; pp 15–18.

(11) Ramos, A.; Morgan, H.; Green, N. G.; Castellanos, A. *J. Phys. D: Appl. Phys.* **1998**, *31*, 2338–2353.

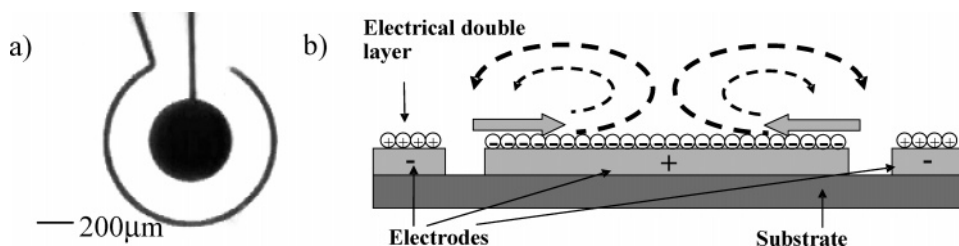


Figure 1. (a) Electrode design of the ac electroosmotic processor (top view). (b) Schematic (side view) illustrating electrode polarization and formation of ac electroosmotic flow. Solid arrows represent the ac electroosmotic force and dotted lines indicate the flow pattern.

allow trapping of the particles into a small region on the electrode surface. The electrokinetic forces, such as DEP and electrophoresis, are especially effective near the electrode surfaces. Therefore, bioparticles can be effectively concentrated into a small region by a combination of fluid flow and particle trapping force.

Manipulations of bioparticles, such as cells, virus, proteins, and DNA molecules, with DEP forces have been reported by different research groups.^{12–18} Our devices are different in several aspects. In a typical DEP concentrator, small electrodes and high voltage are used to generate adequate electric field (in the order of 0.1–1 MV/m). However, the force is only effective near the edges of the electrode due to the rapid decay of the electric potential. Ac electroosmosis requires only a low applied voltage, meaning only a few volts, and can generate bulk fluid motion. The fluid flow significantly increases the effective range of the concentrating process. Furthermore, multiple arrays of electrodes were commonly used in previous studies, and the targets were concentrated throughout the edge of the electrodes. Our device, on the other hand, concentrates the target samples into a small region in the center of the electrode surface, which is advantageous for a downstream sample preparation or detection process. In addition, our device takes advantage of the hydrodynamic flow that is effective for different sizes of objects while maintaining the selectivity of electrokinetic forces to the targets (size and electrical properties). A large variety of biological samples can be concentrated on the same device by just changing the operating parameters. Recently, Hoettges et al.¹⁹ have demonstrated particle concentration with a combination of electrohydrodynamic flow and dielectrophoresis. Since the particles are collected at the center of the metal electrodes instead of the electrode edges, their technique is able to improve the performance of an evanescent light scattering detection system.²⁰ DEP force, however, becomes ineffective for smaller biomolecules due to the strong size dependence of DEP force. In this work, we demonstrate small biomolecules (on the order of nanometer in size) can be

concentrated with a combination of electrophoresis and ac electroosmosis.

The purpose of this paper is to demonstrate the use of electrophoretic, ac electroosmotic, and DEP force for collecting and trapping a large range of biological entities (from nanometer to micrometer range). Particle image velocimetry (PIV) is used to characterize the bulk fluid flow driven by ac electroosmotic force. Understanding this flow mechanism helps to optimize the operating parameters of the bioconcentrator. Experimental results are presented to demonstrate concentration of different bioparticles, such as bacteria and DNA molecules. In addition, we report an interesting behavior of decrease in DNA concentration on the electrode surface at low frequency.

EXPERIMENTAL SECTION

Instruments. The electrodes for generating ac electroosmotic flow were fabricated on microscope slides. Photolithography was done to pattern photoresist on the glass substrate. A 3000-Å-thick gold layer with a 200-Å-thick chromium adhesion layer was evaporated on the glass substrate and patterned by liftoff. Spacers of 125 μm were placed on the chip to define the height of the fluid chamber. The bioprocessor was covered by a coverslip during the experiment. The bioprocessor design consists of a central electrode surrounded by an outer electrode. Figure 1a shows the bioprocessor design. Two sizes of electrodes (outer electrode diameters of 0.65 and 1 mm) were used in this study. A function generator (HP, 33120A) was used to provide the ac signal. The electric distribution was estimated by numerical simulation (CFDRC CFD-ACE+). The chip was loaded onto an epifluorescence microscope (Nikon TE200). The dynamic of molecules and particles were recorded by an intensified CCD camera (Videoscope, ICCD-350F) and directly digitized into a video capture system (Pinnacle, PCTV). All the experiments were performed at room temperature (22–24 °C).

Samples and Preparation. *Escherichia coli* bacteria (XL1-Blue), double-stranded λ phage DNA (48.5 kbp) (Sigma, D3779), and single-stranded DNA (ssDNA) fragments (20 and 50 bases) (MWG Inc.) were used in this study. The radius of gyration of 20- and 50-base ssDNA are 3 and 5 nm, respectively.²¹ The ssDNA fragments were modified with rhodamine red at the 5' end. YoYo-1 (Molecular Probe, Y-3601) was used to label the double-stranded λ phage DNA at a dye-to-base pair ratio of 1:5. The DNA–dye complex was allowed to equilibrate for >1 h before performing the experiment. The conductivity of the medium was adjusted by addition of Tris-EDTA buffer (Sigma, T-9285).

(12) Washizu, M.; Kurosawa, O. *IEEE Trans. Ind. Appl.* **1990**, *26*, 1165–1172.
 (13) Washizu, M.; Suzuki, S.; Kurosawa, O.; Nishizaka, T.; Shinohara, T. *IEEE Trans. Ind. Appl.* **1994**, *30*, 835–843.
 (14) Asbury, C. L.; van den Engh, G. *Biophys. J.* **1998**, *74*, 1024–1030.
 (15) Suehiro, J.; Pethig, R. *J. Phys. D: Appl. Phys.* **1998**, *31*, 3298–3305.
 (16) Hughes, M. P.; Morgan, H.; Rixon, F. J. *Eur. Biophys. J.* **2001**, *30*, 268–272.
 (17) Chou, C.-F.; Tegenfeldt, J. O.; Bakajin, O.; Chan, S. S.; Cox, E. C.; Darnton, N.; Duke, T.; Austin, R. H. *Biophys. J.* **2002**, *83*, 2170–2179.
 (18) Germishuizen, W. A.; Wälti, C.; Wirtz, R.; Johnston, M. B.; Pepper, M.; Davies, A. G.; Middelberg, A. P. J. *Nanotechnology* **2003**, *14*, 896–902.
 (19) Hoettges, K. F.; McDonnell, M. B.; Hughes, M. P. *J. Phys. D: Appl. Phys.* **2003**, *20*, L101–L104.
 (20) Hoettges, K. F.; Hughes, M. P.; Cotton, A.; Hopkins, N. A. E.; McDonnell, M. B. *IEEE Eng. Med. Biol. Mag.* **2003**, *22*, 68–74.

(21) Nkodo, A. E.; Garnier, J. M.; Tinland, B.; Ren, H.; Desruisseaux, C.; McCormick, L. C.; Drouin, G.; Slater, G. W. *Electrophoresis* **2001**, *22*, 2424–2432.

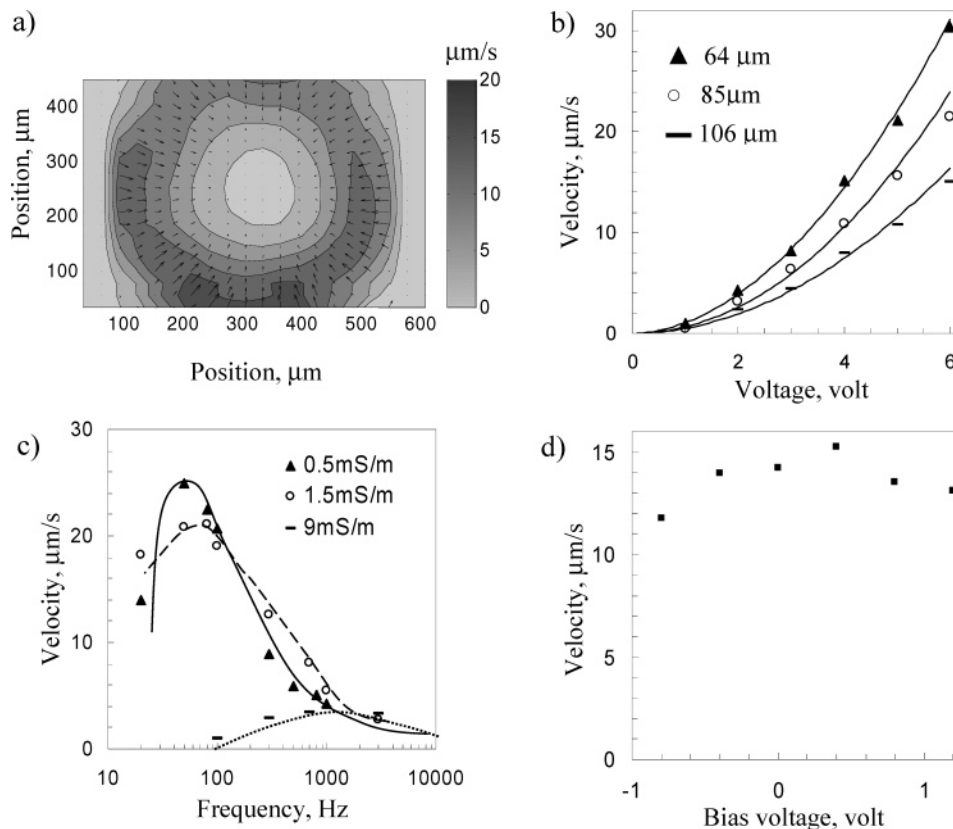


Figure 2. Particle image velocimetry measurement. (a) Velocity distribution above the surface of the central electrode. (b) Voltage dependence of ac electroosmotic velocity measured at three different locations away from the electrode edge. (c) Frequency dependence of ac electroosmotic velocity at different buffer conductivities. (d) Influence of the bias voltage on ac electroosmotic velocity. All the values are measured at a location $\sim 60 \mu\text{m}$ away from the electrode edge.

Particle Image Velocimetry. To measure the fluid velocity generated by ac electroosmosis, we developed a PIV system following Santiago et al.^{22–24} We seeded the fluid with 200-nm fluorescent latex particles (Duke Scientific, R200). The particles were diluted with deionized water such that the concentration was suitable for PIV. The motions of the particles were captured, and the digitized images were analyzed by a cross correlation-based PIV software (TSI, Insight). We averaged at least 20 sets of images for each measurement to minimize variation in the velocity related to random Brownian motion of the submicrometer particles.

RESULTS AND DISCUSSION

Ac Electroosmosis. Our device exploits a combination of ac electroosmosis, electrophoresis, and dielectrophoresis for concentrating biological objects. Ac electroosmosis can transport the particles from a large region in the bulk fluid to the electrode surface. The characteristics of the ac electroosmotic flow are important for optimizing the operating parameters of the concentrator. Therefore, we have performed PIV measurements to characterize the flow properties, such as the flow pattern on the electrode and the frequency dependence, in our electrode design. The velocity component parallel to the central electrode surface was measured by particle image velocimetry (Figure 2a). It is

observed that the electroosmotic flow is fastest near the electrode edge and quickly drops toward the center of the inner electrode. The reduced velocity in the upper region of the electrode is due to the open region of the outer electrode for electrical connection (Figure 1a).

The voltage dependence on the ac electroosmotic flow was measured (Figure 2b). The frequency was fixed at 100 Hz, and the conductivity of the medium was 0.2 mS/m. The velocities of the fluid flow at different applied voltages were measured at three different locations, which were roughly 64, 85, and 106 μm away from the electrode edge. The velocities were fitted by power law with the method of least squares. The exponents are determined to be 1.90, 2.03, and 1.95, respectively. Theory²⁵ predicts that the ac electroosmotic velocity increases with the second power of the applied voltage. Our observation agrees with this theory. It indicates that the bulk fluid flow observed is dominated by ac electroosmosis instead of other electrohydrodynamic flow, such as electrothermal flow (which has a fourth power dependence).^{11,26} Ac electroosmotic flow is sensitive to the applied frequency and conductivity of the medium (Figure 2c). For instance, the ac electroosmotic velocity tends to be zero at high- and low-frequency limits and has a maximum at an intermediate frequency. Furthermore, the frequency maximum increases with the conductivity of the medium. The frequency dependence is consistent with other

(22) Santiago, J. G.; Wereley, S. T.; Meinhart, C. D.; Beebe, D. J.; Adrian, R. J. *Exp. Fluids* **1998**, *25*, 316–319.

(23) Meinhart, C. D.; Wereley, S. T.; Santiago, J. G. *Exp. Fluids* **1999**, *27*, 414–419.

(24) Wong, P. K.; Lee, Y.-K.; Ho, C.-M. *J. Fluid Mech.* **2003**, *497*, 55–65.

(25) Ramos, A.; Morgan, H.; Green, N. G.; Castellanos, A. *J. Colloid Interface Sci.* **1999**, *217*, 420–422.

(26) Green, N. G.; Ramos, A.; González, A.; Castellanos, A.; Morgan, H. *J. Phys. D: Appl. Phys.* **2000**, *33*, L13–L17.

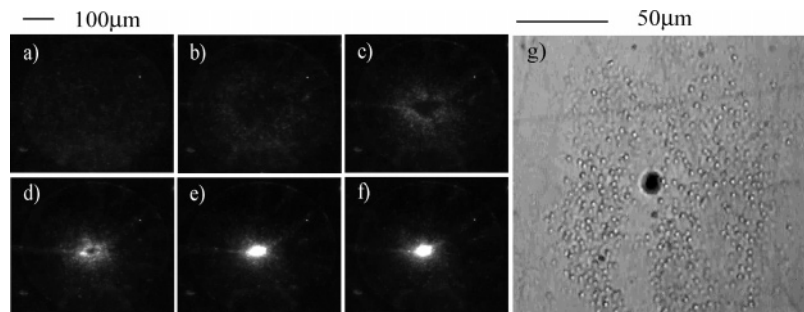


Figure 3. Particle concentration. (a–f) Video time series showing concentration of 200-nm fluorescence particles on the central electrode. Each picture is separated by 10 s. (g) Concentration of *E. coli* bacteria at the center of the central electrode.

researchers' results obtained by tracking individual particles on parallel electrodes.²⁷ The strong frequency dependence of the ac electroosmosis allows tuning of the strength of the ac electroosmosis relative to other electrokinetic forces, which is essential for concentrating the bioparticles.

Electrophoretic Force. Ac electroosmosis can transport small molecules from the bulk fluid to the region near the electrode. However, it is not able to trap the target molecules. To concentrate the particles, a trapping force is required to capture the molecules on the electrode surface. Electrophoretic force is effective for manipulating charged particles, such as negatively charged DNA molecules, in microscale.⁷ Electrophoresis describes the movement of charged particles in a liquid medium under an external electric field. When a particle with charge q is under a steady electric field E , the particle experiences an electrostatic force qE . To capture the DNA molecules on the electrode surface, the electrophoretic force should balance the hydrodynamic drag force generated by ac electroosmosis. The condition is given by

$$qE \geq 6\pi r\mu v_m$$

where r is particle radius, μ is the viscosity of the medium, and v_m is the velocity of the medium.

To generate an electrophoretic force for trapping charged molecules, we applied a dc offset voltage in the ac signal. The time-averaged electrophoretic force is proportional to the dc bias voltage while the ac electroosmosis increases with the second power of the applied ac voltage (Figure 2b). Therefore, the relative strength of the hydrodynamic drag force and electrophoretic force can be adjusted independently with dc bias, ac signal, and applied frequency (Figure 2c). We have also characterized the effect of the bias voltage on the ac electroosmotic velocity (Figure 2d). We applied an ac voltage of 4 V (peak to peak) at 100 Hz and measured the ac electroosmotic velocities at different bias voltages. The dc offset shows only moderate effect ($\pm 15\%$) on the ac electroosmotic velocity within the range we tested.

Dielectrophoretic Force. It should be noted that the observed velocity of the particle is a combined effect of the hydrodynamic drag force produced by the ac electroosmotic field and the DEP force.^{28,29} In the given experimental condition, the particles should display positive DEP, by which the particles are attracted toward the electrode edges (opposite to the direction of the particle

motion observed). It indicates that the electrohydrodynamic flow is stronger than the DEP force at the given condition. Balancing DEP force with Stokes drag provides a rough estimation of the influence of DEP force to the particle's velocity.

$$2\pi r^3 \epsilon_m \text{Re}\{K(\omega)\} \nabla |E_{\text{rms}}|^2 = 6\pi r\mu (v_m - v_p)$$

where ϵ_m is the permittivity of the medium, $\text{Re}\{K(\omega)\}$ represents the real part of the Clausius–Mossotti factor at angular frequency ω , E_{rms} is the root-mean-square electric field, and v_p is the velocity of the particle. The term $\text{Re}\{K(\omega)\}$ is bounded by -0.5 and 1 and is assumed to be 1 for order of magnitude estimation. The electric field distribution can be calculated by numerical simulation. The term $\nabla |E_{\text{rms}}|^2$ is estimated to be $\sim 10^{12} \text{ V}^2 \text{ m}^{-3}$ near the edge of the electrode and 10^7 – $10^8 \text{ V}^2 \text{ m}^{-3}$ at the locations where velocities are measured. It reveals that the DEP force has negligible effect on our velocity measurement at the given experimental condition. However, it is not correct in general, especially near the edge of the electrode where the DEP force can increase several orders of magnitude. It has been proven that the DEP force can affect the measurement of the electrohydrodynamic flow.²⁸ More accurate fluid velocity estimation can be obtained by performing the measurement with two different sizes of particles.²⁸

Concentration of Particles. To investigate the concentration process, we observed the behavior of 200-nm fluorescent particles at different applied frequencies. The diameter of the outer electrode was ~ 1 mm, and the conductivity of the medium was 1.5 mS/m . The particles were concentrated at a voltage of 8 V and 1 kHz . We observed the particles aggregated and moved toward the center of the electrode. The particles concentrated into a small region less than $100 \mu\text{m}$ in diameter in less than 1 min (Figure 3a–f). The concentration process can be understood by the combined effect of ac electroosmosis and dielectrophoresis. However, other electrokinetic effects may also contribute to the observed particle trapping. The existence of the particles can introduce inhomogeneities in the electric double layer (EDL) on the electrode surface, which causes more complex particle–electrode interactions.^{30,31} In addition to the interaction between

(27) Green, N. G.; Ramos, A.; González, A.; Morgan, H.; Castellanos, A. *Phys. Rev. E* **2000**, *61*, 4011–4018.

(28) Meinhart, C. D.; Wang, D.; Turner, K. *Biomed. Microdevices* **2003**, *5*, 139–145.

(29) Green, N. G.; Ramos, A.; Morgan, H. *J. Phys. D: Appl. Phys.* **2000**, *33*, 632–641.

(30) Jones, T. B. *Electromechanics of Particles*; Cambridge University Press: New York, 1995.

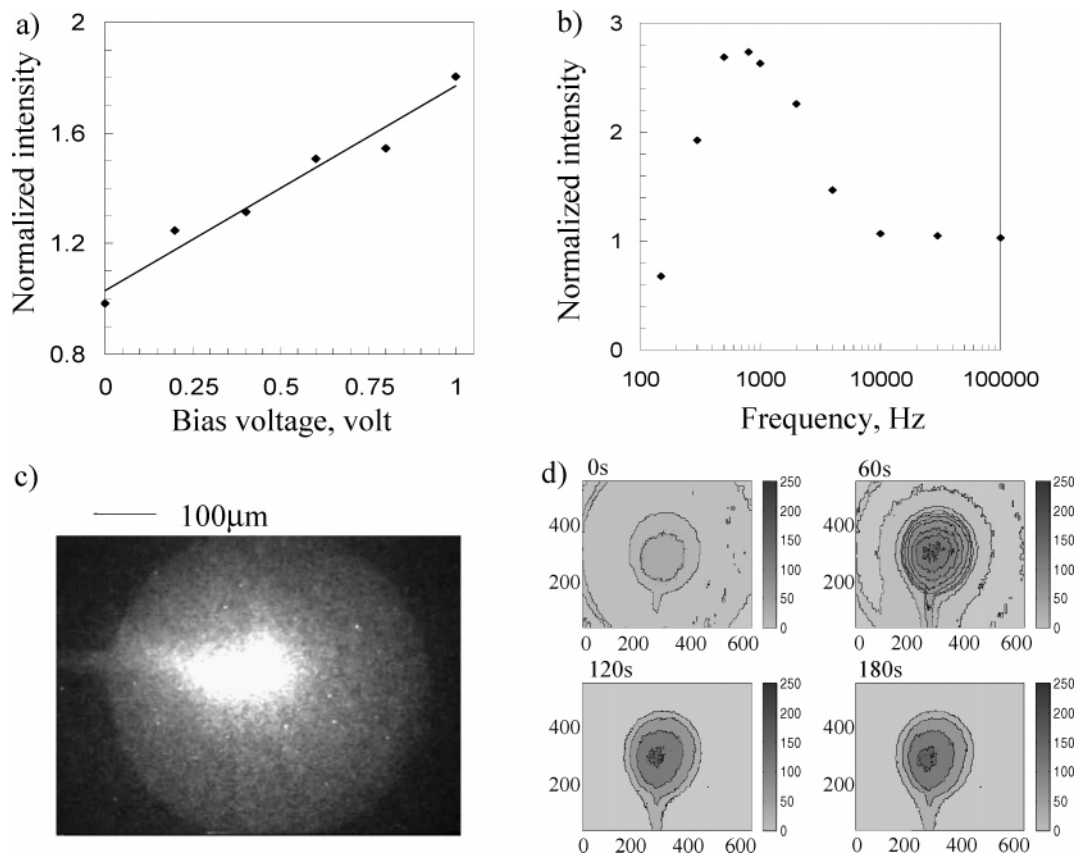


Figure 4. Concentration of DNA molecules. The dependence of (a) bias voltage and (b) frequency for concentrating ssDNA fragments (20 bases). Intensities are measured at the center of the central electrode surface after applying the potential for 80 s. (c) Fluorescence picture demonstrating concentration of double-stranded λ phage DNA molecules (48.5 kbp) on the central electrode. (d) Concentration of ssDNA fragments (20 bases). The contours indicate the intensity, i.e., the concentration, of the molecules at different times. Dimensions are in micrometers.

the particles and the electrodes, aggregation and pearl chain formation of particles are frequently observed during electrokinetic manipulations. The particle–particle mutual attraction is a result of dipole–dipole interactions and the local distortion of the electric field due to the existence of the particles.³⁰ This may also contribute to the particle trapping.

We have applied the same trapping effect for concentrating *Escherichia coli* bacteria. The conductivity of the medium was 13.0 mS/m. The *E. coli* bacteria can be concentrated with an applied frequency of 1–2 kHz. In general, the trapping force for *E. coli* is stronger compared to trapping of the 200-nm particle. It can be explained by the larger size of the bacteria ($\sim 1\text{--}2\ \mu\text{m}$) as the DEP is very sensitive to the size of the object. Moreover, the bacteria moved slower compared to the motion of 200-nm particles, which is likely due to the higher conductivity of the medium. Roughly 3 min was required to concentrate the bacteria at 8 V. Higher voltage (14 V) can be applied to shorten the time required. Figure 3b shows *E. coli* concentrated at the electrode surface after applying electric potential for 1 min. Similar aggregations have been reported for yeast cells during DEP manipulation with interdigitated castellated electrodes³² and for submicrometer particles during ac electroosmosis experiments with parallel electrodes.³³ Particle concentration has also been demonstrated for yeast cells, *Bacillus subtilis var niger* spores, and 110-nm

fluorescently labeled latex beads using an interlocking circular electrode design.¹⁹ Our results of particle visualization and concentration form the basis for concentrating a wide range of biological objects, where other electrokinetic forces can be combined with ac electroosmosis. The PIV measurement can serve as a guide for selecting the operating parameters, such as conductivity of the medium, applied voltage, and frequency. With this bioprocessor design, we have demonstrated concentration of *E. coli* from a region of $\sim 1\ \text{mm}$ into an area less than $100\ \mu\text{m}$ in diameter.

Concentration of Biomolecules. Concentration of small biomolecules is always needed to increase the signal level of biomarker sensors. However, the difficulty increases with decreasing size of the molecules. We found that the small molecules can be concentrated by applying a dc bias in the ac signal. The effect of dc bias on the concentration of DNA molecules (single-stranded 20 bases) was measured. Neutral density filters were used to reduce the illumination intensity, which minimized photobleaching. As verified by the control experiment, photobleaching was negligible in the experimental condition (data not shown). The conductivity of the medium was 12.0 mS/m. We applied 4 V (peak to peak) at 800 Hz. Figure 4a shows the intensity at the center of the electrode after 80 s under different bias voltage. The intensities were normalized by the initial intensity. There was no significant change in the intensity when zero bias was applied and the

(31) Trau, M.; Saville, D. A.; Aksay, I. A. *Science* **1996**, *272*, 706–709.

(32) Pethig, R.; Huang, Y.; Wang, X.-B.; Burt, J. P. H. *J. Phys. D: Appl. Phys.* **1992**, *25*, 881–888.

(33) Green, N. G.; Ramos, A.; González, A.; Morgan, H.; Castellanos, A. *Phys. Rev. E* **2002**, *66*, 026305.

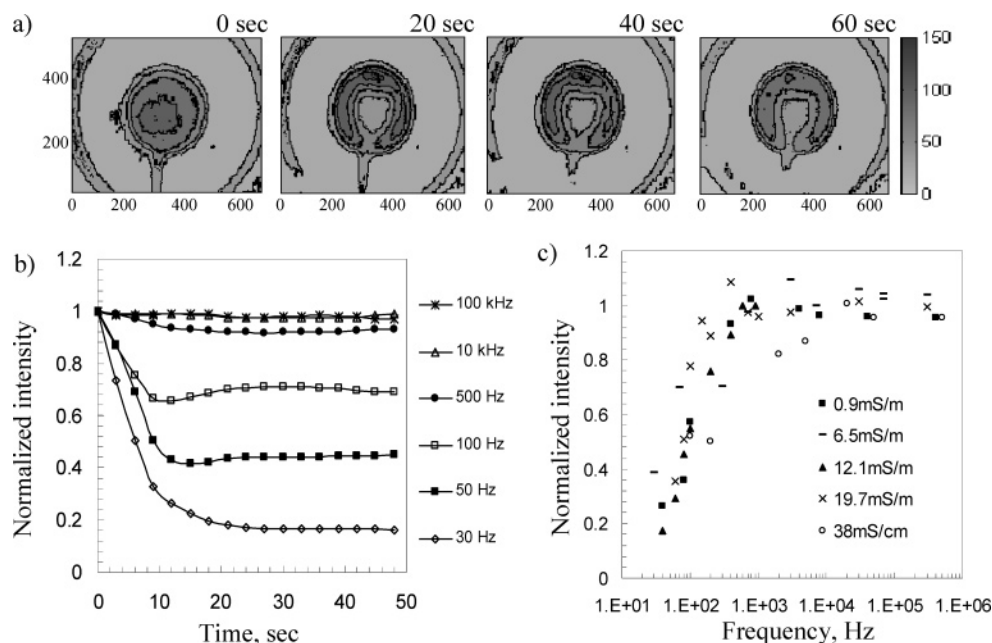


Figure 5. DNA concentration under pure oscillating electric field. (a) Intensity distribution on the electrode surface at different time. Dimensions are in micrometers. (b) Intensities at the center of the electrode with different applied frequency. (c) Frequency dependence of the phenomenon measured at different buffer conductivities. All the values are measured after the application of the potential for 1 min.

intensity increased with the bias voltage in the range tested. Furthermore, we have measured the frequency dependence of concentration of DNA molecules (Figure 4b). The bias voltage was 1 V. The frequency dependence was similar to ac electroosmosis. The maximum effect occurred at an intermediate frequency. The peak frequency was ~ 1 kHz, and the effect became negligible when the frequency was higher than 10 kHz. Unexpectedly, the intensity was lower than the original value when the applied frequency was lower than 200 Hz. Figure 4c shows the fluorescence picture of double-stranded λ -phage DNA concentrated on the electrode surface. DNA molecules were concentrated on the electrode surface by applying 4 V at 1 kHz with a 1-V bias. The conductivity of the medium was 15.0 mS/m. Figure 4d illustrates the concentration of the 20-base single-stranded DNA molecules. The contours indicate the intensities at different locations. The DNA molecules were concentrated within 3 min.

Although DEP force can concentrate bioparticles in micrometer and submicrometer range, it is difficult to manipulate smaller biomolecules efficiently. In our experiment, there is no concentration of the molecules observed at the edges when an oscillating potential with a zero mean value was applied. It is expected, as the DEP force decreases rapidly (to the third power) with the particle size.³⁴ Moreover, large electrode size is used in this study to concentrate samples from a large region (~ 1 mm). The electric field strength was on the order of 10 kV m^{-1} compared to $0.1\text{--}1 \text{ MV m}^{-1}$ used in other DNA trapping experiments.^{12,14,17,18} The observed results can be explained by the charge property of the DNA molecules, which are negatively charged. When a charged particle is under an external electric field, the particle experiences an electrophoretic force. In pure oscillating potentials without dc offset, there is no net movement of the particles. If there is an offset in the ac signal, the time-averaged electrophoretic force is

nonzero and the force increases with the bias voltage. It is in agreement with the experimental observation that there was no concentration of the DNA molecules at zero bias and that trapping of molecules increased with the bias voltage. Therefore, the trapping of the DNA molecules was likely to be the result of the electrophoretic force. On the other hand, the frequency dependence of concentrating DNA molecules was consistent with the ac electroosmotic flow. The peak frequency for the concentration of DNA molecules was the same as the peak frequency for ac electroosmosis at a similar conductivity. It should be noted that there is no observable concentration of the molecules when only a dc voltage was applied. The result indicates that ac electroosmosis was required for the concentration of the DNA molecules. Another possible effect is that ac electric field minimizes the effect of electrode polarization^{35,36} and maximizes the effective electric field strength. However, the decrease of the concentration effect at a frequency higher than 1 kHz cannot be explained by electrode polarization. The effect of electrode polarization should decrease with increasing frequency. Therefore, electrode polarization cannot be a dominant factor for the concentration of the molecules; however, it could be responsible for the observed effect at pure dc voltage. Our results show that a combination of ac electroosmosis and the electrophoresis was able to concentrate the DNA molecules. The electrophoretic force played a role similar to that of the DEP force in trapping micrometer and submicrometer particles.

Defocusing of DNA Molecules. As found in the measurements with varying frequencies, there was a decrease of intensity, which indicates a decrease in DNA concentration at the center of the central electrode at low frequency (< 200 Hz). To characterize

(34) Pohl, H. A. *Dielectrophoresis*; Cambridge University Press: Cambridge, U.K., 1978.

(35) Feldman, Yu.; Polygalov, E.; Ermolina, I.; Polevaya, Yu.; Tsentsiper, B. *Meas. Sci. Technol.* **2001**, *12*, 1355–1364.

(36) Gunning, J.; Chan, D. Y. C.; White, L. R. *J. Colloid Interface Sci.* **1995**, *170*, 522–537.

this phenomenon (decrease of intensity at the center of the electrode), pure oscillating potential of 6 V (peak to peak) at 70 Hz was applied. The conductivity of the medium was 7.6 mS/m. Figure 5a shows the intensity distribution on the electrode surface at different times. The concentration of the ssDNA molecules at the center of the electrode reached steady state within 20 s. It is possible that the DNA molecules at the center were pushed toward the edge. The intensity near the edge of the electrode decreased slowly. Figure 5b shows the intensity at the center of the electrode with different applied frequency. Below 400 Hz, the phenomenon became stronger as frequency decreased. We also performed the experiment with different buffer conductivities. Figure 5c shows the intensity at the center of the central electrode after the application of the potential for 1 min.

The physical origin of the phenomenon is unclear at the moment. Electrohydrodynamic flow, such as ac electroosmosis and electrothermal flow,^{7,11} is not likely to be important because the phenomenon has different frequency dependency and sensitivity to the conductivity of the medium. More importantly, pure electrohydrodynamic flow cannot induce the local concentration distribution from the initial uniform distribution of the DNA molecules. A local force that exerts effect on embedded molecules should be responsible for the observation. Dielectrophoresis of DNA molecules (as small as 368 bp for dsDNA and 1137 bases for ssDNA) has been demonstrated to be feasible.^{12,14,17} Positive dielectrophoresis has been reported for manipulating λ phage DNA at a similar condition.¹⁴ Below 1 kHz, they observed comparable frequency dependency. Larger voltage is required to trap the λ phage DNA molecules at higher frequencies. However, we did not observe accumulation of the molecules at the edge of the electrode for the entire range of frequencies tested (30–300 kHz). On the contrary, the intensity near the edge of the electrode decreases with time. Neither positive DEP nor negative DEP is able to explain the observed intensity distribution. In either case, the effect should be strongest at the edge, where the electric field gradient is highest. However, we do not exclude the possibility that the observed phenomenon is due to a combination of DEP

force with other electrokinetic forces. On the other hand, the interaction between the DNA molecules and the EDL on the electrode surface may have contributed to the phenomenon.^{31,37} The frequency dependence of the phenomenon is consistent with the EDL formation. The influence of the EDL is expected to be stronger at lower frequency. It should also be noted that the intensity was almost constant at the surface of the outer electrode, which has relatively small surface area. However, there is no direct evidence showing that the observation was a result of the molecule–electrode interaction. Further investigation is required to understand this interesting observation.

CONCLUSION

We have developed an electrokinetic processor for concentrating biological samples in a microbioanalysis system. A combination of particle trapping force and the electrohydrodynamic flow has successfully concentrated various bioparticles from micrometer to nanometer in size. With electrophoretic forces generated by a dc offset, we are able to concentrate ssDNA molecules as small as 20 bases, which are commonly used in biotechnology protocols (e.g., PCR, hybridization assay, and microarray). We have also observed a decrease in DNA concentration on the electrode surface at low frequency. This interesting behavior is not clearly understood and cannot be explained by any known electrokinetic forces. This phenomenon has a large effective range and only requires small driving voltage. This interesting finding can potentially be applied to applications, such as stringency control or diffusivity measurement (similar to fluorescence recovery after photobleaching).

ACKNOWLEDGMENT

The authors thank Dr. Joanne H. Deval for her valuable discussion and Wilson WaiChun Wong for providing the bacteria samples. This work is supported by CMISE through NASA URETI program and NIH NIDCR (UO1 DE15018).

Received for review April 4, 2004. Accepted September 10, 2004.

AC049479U

(37) Yeh, S.-R.; Seul, M.; Shraiman, B. I. *Nature* **1997**, *386*, 57–59.